J Eng Math (2008) 60:89–100
DOI 10.1007/s10665-007-9138-6

Wall slip induced by a micropolar fluid

Guy Bayada · Nadia Benhaboucha · Michèle Chambat

Received: 15 June 2005 / Accepted: 24 January 2007 / Published online: 11 September 2007

Abstract Lubrication theory is devoted to the study of thin-film flows, More often, the fluid can be considered as a Newtonian one and no-slip boundary conditions can be retained for the velocity at the fluid solid interface. With these assumptions it is possible to deduce from the (Navier) Stokes system a simplified equation describing the flow: the Reynolds equation. It allows to compute the pressure distribution inside the film and to obtain overall performances of a lubricated device such as load and friction coefficient. For very thin films, however, surface effects at the fluid solid interface become very important and no-slip conditions cannot be retained. Solid surfaces exert some influence on the liquid molecules and the effective shear viscosity along the boundary differs from the classical bulk shear viscosity. Moreover, the microstructure of the fluid cannot be ignored, especially the effects of solid-particle additives in the lubricant. Micropolar theory for fluids is often adopted to account of such microstructure and microrotation. In the present study, a thin micropolar fluid model with new boundary conditions at the fluid–solid interface is considered. This condition links velocity and microrotation at the interface by introducing a so-called "boundary viscosity". By way of asymptotic analysis, a generalized micropolar Reynolds equation is obtained. Numerical results show the influence of the new boundary conditions for the load and friction coefficients. Comparisons are made with other works that retain the no-slip boundary conditions.

Keywords Boundary viscosity · Lubrication · Micropolar fluid · Reynolds equation · Slippage effect

1 Introduction

Studies related to lubricated devices in which the gap between the moving surfaces decreases to molecular dimensions concern both experimental and theoretical aspects. Experimental results [1–7] show that the solid-surface

G. Bayada
CNRS UMR 5208-5259, INSA de Lyon, Bât 401, Villeurbanne 69621, France
e-mail: Guy.Bayada@insa-lyon.fr

N. Benhaboucha (✉) · M. Chambat
CNRS UMR 5585, Univ. Lyon 1, Maply, Bât J. Braconnier, Villeurbanne 69622, France
e-mail: benhabouc@maply.univ-lyon1.fr

M. Chambat
e-mail: chambat@maply.univ-lyon1.fr

force exerts some influence on the liquid molecules and that the effective shear viscosity along the boundary differs from the classical bulk shear viscosity. This difference seems to be strongly connected with the nature of the solid surface [8,9].

A possible way to introduce such experimental facts which retain the suitability of a continuum-mechanical approach is to use micropolar fluid-film theory. Introduced by Eringen [10], it concerns a classs of fluids with a microsturucture in which each element can translate or rotate and deform. Later, a simplified theory in which deformation is ignored was proposed by Eringen [11] and Aero [12]. These equations are a generalization of the (Newtonian) Navier–Stokes equations and deal with three fields, velocity u, pressure p and microrotation ω, together with some viscosity parameters and material constants to describe the behaviour of the fluid.

The micropolar equations are

$$-(\nu + \nu_\gamma)\Delta u + \rho(u.\nabla)u + \nabla p = 2\nu_\gamma(\nabla \times \omega), \tag{1}$$

$$-(c_a + c_d)\Delta\omega + \rho j(u.\nabla)\omega + 4\nu_\gamma\omega = 2\nu_\gamma(\nabla \times u), \tag{2}$$

$$\text{div } u = 0. \tag{3}$$

The quantities ν, ν_γ, c_a, c_d are different viscosities that characterize the isotrophic properties of the fluid [11–13], ρ is the mass density and j is a micro-inertia constant.

As it is well known, reasonable boundary conditions have to be specified on velocity and microrotation for solving such equations. While the no-slip condition is widely used for velocity, the situation is not so clear for microrotation. In most of the previously mentioned references, a zero boundary condition for microrotation is more or less explicitly assumed. If s is the given velocity of the wall, these conditions are written:

$$u = s = (s_1, s_2) \tag{4}$$

$$\omega = 0. \tag{5}$$

Using this set of boundary conditions, micropolar models have been widely used in tribology [11,14–18]. In these papers, detailed equations are given as well as the procedure to obtain a generalized 1D or 2D Reynolds equation from the 2D or 3D (Navier) Stokes micropolar equations (1–3)

It was pointed out in [19], see also [20], that another boundary condition can be used for microrotation. Following [21,22] it is proposed to link the value of the micorotation with the rotation of the velocity by way of a coefficient α that characterizes the microrotation on the solid surfaces and is computed from a boundary viscosity value,

$$\omega \times n = \frac{\alpha}{2}(\nabla \times u) \times n, \tag{6}$$

in which n is a normal unit vector to the boundary.

Using conditions (4–6), a "new" generalized micropolar Reynolds equation (30) is derived. Numerical calculations show the importance of the new parameter α for the performance of lubricated devices for both load and friction.

However, a mathematical study of the micropolar equations (1–3) has shown [23] that it is not possible to consider boundary conditions such as (6) and to simultaneously retain the no-slip condition (4) for the velocity. This would be like simultaneously considering, at the same boundary, a Neumann and a Dirichlet boundary condition. A mathematical choice of velocity condition compatible with (6) can be obtained by using a variational formulation for the problem (1–3). This condition allows a slippage in the tangential direction and retains a non-peneration condition in the normal direction n (δ_0 is a real parameter)

$$(u - s) \times n = \delta_0(\nabla \times \omega) \times n \quad \text{and} \quad u \cdot n = 0. \tag{7}$$

Let us mention that in most lubrication studies, it is assumed that the speed of the lubricant at the surface equals that of the solid surface. However, it has been found that wall slip occurs, not only in non-Newtonian flows [24–29], but also in hydrodynamic lubrication or elasto-hydrodynamic lubrication [30–33]. It seems that such a phenomenon is linked to physical or chemical interactions of the solid surfaces with the lubricant. Various boundary conditions have been considered in these works to model this type of slippage. Most of them included limited yield stress or retain a slippage value proportional to the shear stress.

Condition (7) seems to be a new one directly linked to the introduction of the microrotation field ω. We show how it is possible to obtain a thin-film Reynolds equation taking such boundary conditions into account and we give some numerical results to show the fluid slippage at the wall. It is of particular interest to show that the slippage induces a weaker load than that of Bessonov's model [34] in which no-slip boundary conditions have been retained.

2 Boundary conditions and governing equations

To state the lubrication assumptions, a 3D device is considered and the fluid domain is defined by

$$E = \{(x, y, z); (x, y) \in \mathrm{w}, 0 < z < h(x, y)\}, \tag{8}$$

where h is the film thickness, and w is a subset of the plane (x, y).

Let Γ_3, Γ_1 be the upper and lower boundaries of E (see Fig.1)

Recalling that $\varphi = (\varphi_1, \varphi_2, \varphi_3)$

$$\nabla \times \varphi = \left(\frac{\partial \varphi_3}{\partial \mathrm{y}} - \frac{\partial \varphi_2}{\partial z}, \frac{\partial \varphi_3}{\partial x} + \frac{\partial \varphi_1}{\partial z}, \frac{\partial \varphi_2}{\partial x} - \frac{\partial \varphi_1}{\partial \mathrm{y}} \right), \tag{9}$$

one has the corresponding equations (1–3). The usual boundary conditions for the velocity and microrotation are assumed on Γ_3

$$u = 0 \quad \text{on } \Gamma_3, \tag{10}$$

$$\omega = 0 \quad \text{on } \Gamma_3. \tag{11}$$

On the part Γ_1 of the boundary, which corresponds to the moving boundary, the impermeability of the wall leads to

$$u \cdot n = 0 \quad \text{on } \Gamma_1, \tag{12}$$

$$\omega \cdot n = 0 \quad \text{on } \Gamma_1, \tag{13}$$

associated with the boundary conditions discussed in the Introduction

$$\omega \times n = \frac{\alpha}{2} (\nabla \times u) \times n \text{ on } \Gamma_1, \tag{14}$$

$$(u - s) \times n = \delta_0 (\nabla \times \omega) \times n \text{ on } \Gamma_1, \tag{15}$$

In [19], it was proposed to define the parameter α as a microrotation retardation at the boundary and to connect it with the different viscosity coefficients. It has been shown experimentally [35,36] that there are chemical interactions between a solid surface and the nearest fluid layer. This has to be taken into account, especially for a non-Newtonian fluid and a very thin-film thickness. This can be done by introducing a viscosity ν_b near the surface which is different form ν and ν_γ. In [19], it was proposed to define α by means of this "boundary viscosity" ν_b by

$$\alpha = \frac{\nu + \nu_\gamma - \nu_b}{\nu_\gamma}. \tag{16}$$

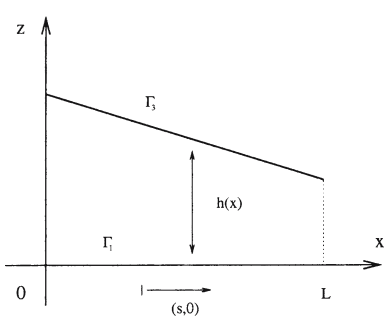

Fig. 1 Geometry of a slider bearing (Domain E in 2D)

Following [19], it is possible to give physical limits to ν_b, inducing

$$0 \le \nu_b \le \nu + \nu_\gamma \Rightarrow 0 \le \alpha \le \frac{\nu + \nu_\gamma}{\nu_\gamma}. \tag{17}$$

The value $u - s$, if it is not zero, characterises the slippage on Γ_1 and δ_0 is an additional parameter which will enable the influence of this new boundary condition to be controlled.

Let us introduce the dimensionless normalized variables and functions

$$\begin{aligned}
&X = \frac{x}{L}, \quad Y = \frac{y}{L}, \quad Z = \frac{z}{c}, \quad H = \frac{h}{c}, \quad \epsilon = \frac{c}{L},\\
&\bar{u} = \frac{u}{g_0}, \quad \bar{p} = \frac{c^2}{g_0(\nu+\nu_\gamma)L}p, \quad \bar{\omega} = \frac{c}{g_0}\omega, \quad \mathrm{Re} = \frac{\rho g_0 c}{\nu+\nu_\gamma}, \quad \mathrm{Re}' = \frac{\rho j g_0 c}{c_a + c_d},\\
&N^2 = \frac{\nu_\gamma}{\nu+\nu_\gamma}, \quad R_M = \frac{c_a + c_d}{(\nu+\nu_\gamma)c^2}, \quad \bar{s} = \frac{s}{g_0}, \quad \delta = \frac{\delta_0}{c^2}.
\end{aligned} \tag{18}$$

where g_0 is a characteristic velocity of the surface, L a characteristic length of the lubricated area of the device and c that of the film thickness. The usual lubrication assumptions are made to derive the Reynolds equation.

1. Flow is laminar: vortex and turbulence do not occur anywhere in the film.
2. Body forces are neglected, e.g. the gravitational force and the magnetic field are assumed to be negligible.
3. The film is sufficiently thin compared with the length and the span of the bearing to allow the curvature of the fluid film to be ignored. The rotational velocities may be replaced by translational velocities ($h \ll L$)

Re is the modified Reynolds number where ν has been replaced by $\nu + \nu_\gamma$ and this number is always smaller than the classical Reynolds number. For lubrication problems $\mathrm{Re} \ll 1$ and is generally of the order of 10^{-3}. Also it is reasonable to assume that $\mathrm{Re}' \ll 1$.

Further, ϵ is small, of the order of 10^{-3}. Using these assumptions and the previous requirements, Eqs. 1–3 reduce to

$$-\frac{\partial^2 \bar{u_1}}{\partial Z^2} + \frac{\partial \bar{p}}{\partial X} = -2N^2 \frac{\partial \bar{\omega}_2}{\partial Z}, \tag{19}$$

$$-\frac{\partial^2 \bar{u_2}}{\partial Z^2} + \frac{\partial \bar{p}}{\partial Y} = -2N^2 \frac{\partial \bar{\omega}_1}{\partial Z}, \tag{20}$$

$$-R_M \frac{\partial^2 \overline{\omega}_1}{\partial Z^2} + 4N^2 \overline{\omega}_1 = -2N^2 \frac{\partial \overline{u}_2}{\partial Z}, \tag{21}$$

$$-R_M \frac{\partial^2 \overline{\omega}_2}{\partial Z^2} + 4N^2 \overline{\omega}_2 = 2N^2 \frac{\partial \overline{u}_1}{\partial Z}, \tag{22}$$

$$\frac{\partial \overline{p}}{\partial Z} = 0, \quad \overline{u}_3 = 0, \quad \overline{\omega}_3 = 0, \tag{23}$$

$$\frac{\partial}{\partial X}\left[\int_0^H \overline{u}_1(X,Y,Z)\mathrm{d}Z\right] + \frac{\partial}{\partial Y}\left[\int_0^H \overline{u}_2(X,Y,Z)\mathrm{d}Z\right] = 0, \tag{24}$$

with the boundary conditions

$$\frac{\partial \overline{u}_1}{\partial Z}(X,Y,0) = \frac{2}{\alpha}\overline{\omega}_2(X,Y,0), \tag{25}$$

$$\frac{\partial \overline{u}_2}{\partial Z}(X,Y,0) = -\frac{2}{\alpha}\overline{\omega}_1(X,Y,0), \tag{26}$$

$$\overline{u}_2(X,Y,0) - \overline{s}_2 = \delta \frac{\partial \overline{\omega}_1}{\partial Z}(X,Y,0), \tag{27}$$

$$\overline{u}_1(X,Y,0) - \overline{s}_1 = -\delta \frac{\partial \overline{\omega}_2}{\partial Z}(X,Y,0), \tag{28}$$

$$\overline{u}(X,Y,H) = \overline{\omega}(X,Y,H) = 0. \tag{29}$$

The procedure to obtain a solution to Eqs. 19–22 with boundary conditions (25)–(29) is given in the Appendices 1 and 2. Then, the derived generalized Reynolds equation can be written in the following form

$$\frac{\partial}{\partial X}\left(\Theta_1\frac{\partial \overline{p}}{\partial X}\right)+\frac{\partial}{\partial Y}\left(\Theta_1\frac{\partial \overline{p}}{\partial Y}\right)=\frac{\partial}{\partial X}(\Theta_2\overline{s}_1)+\frac{\partial}{\partial Y}(\Theta_2\overline{s}_2), \tag{30}$$

with, for $\alpha \neq 1$ (see Appendix 1)

$$\Theta_1=\frac{H^3}{3(1-N^2)}+\left[\frac{\gamma_\alpha}{2}H^2-\frac{2N^2}{k}\left(\frac{\cosh(kH)-1}{k}-H\sinh(kH)\right)\right]A_1-\frac{2N^2}{A_1}\left(\frac{\sinh(kH)}{k}-H\cosh(kH)\right)B_1, \tag{31}$$

$$\Theta_2=\left[-\frac{\gamma_\alpha}{2}H^2+\frac{2N^2}{k}\left(\frac{\cosh(kH)-1}{k}-H\sinh(kH)\right)\right]A_2+\frac{2N^2}{k}\left(\frac{\sinh(kH)}{k}-H\cosh(kH)\right)B_2, \tag{32}$$

$$k=2N\sqrt{\frac{1-N^2}{R_M}},\quad \gamma_\alpha=\frac{2(1-\alpha N^2)}{\alpha-1}, \tag{33}$$

and for $\alpha = 1$ (see Appendix 2)

$$\Theta_1=\frac{H^3}{3(1-N^2)}+\frac{H^2}{2(1-N^2)}A_1'-\frac{2N^2}{k}\left(\frac{\sinh(kH)}{k}-H\cosh(kH)\right)B_1', \tag{34}$$

$$\Theta_2=\frac{H^2}{2(1-N^2)}A_2'-\frac{2N^2}{k}\left(\frac{\sinh(kH)}{k}-H\cosh(kH)\right)B_2', \tag{35}$$

(A_i, B_i, A_i', B_i', $i = 1, 2$ are defined in the Appendices 1 and 2).

3 Comparison with previous studies

In this section, we will consider two particular mechanical devices, a slider bearing and a journal bearing. We will show the sensitiveness for two operational parameters: the load W and the friction coefficient c_f. We aim to compare the results obtained with our model with those of [16,34] which are related to infinitely long devices in 2D.

In this case, the pressure is a function of X only and the generalized micropolar Reynolds equation (30) becomes

$$\frac{\partial}{\partial X}\left(\Theta_1\frac{\partial \overline{p}}{\partial X}\right)=\frac{\partial}{\partial X}(\Theta_2\overline{s}_1). \tag{36}$$

3.1 The slider bearing

As a first example, we consider a simple device with a negative slope described in Fig. 1. The film thickness can be written by introducing a parameter m

$$h(x)=c\left(1+m\frac{x}{L}\right),\quad 0<x<L\quad\text{and}\quad m<0. \tag{37}$$

The load W along the moving surface Γ_1 is defined by

$$W=\int_0^L p(x,0)\mathrm{d}x. \tag{38}$$

The shear stress along the surface Γ_1 is

$$(\nu + \nu_\gamma)\frac{\partial u_1}{\partial z}(x,0) - 2\nu_\gamma \omega(x,0). \tag{39}$$

The friction force F is obtained by integrating the shear stress along the moving surface, thus

$$F = \int_0^L \left((\nu + \nu_\gamma)\frac{\partial u_1}{\partial z}(x,0) - 2\nu_\gamma \omega(x,0)\right) \mathrm{d}x. \tag{40}$$

The friction coefficient c_f is determined by

$$c_f = \frac{F}{W}. \tag{41}$$

Using the normalization given in Sect. 2, we define the rescaled film thickness.

$$H(X) = (1 + mX), \quad 0 < x < 1 \quad \text{and} \quad m < 0, \tag{42}$$

and the corresponding $\overline{W}$ and $\overline{F}$

$$\overline{W} = \int_0^1 \overline{p}(X)\mathrm{d}X = \frac{\epsilon^2}{g_0(\nu + \nu_\gamma)} W, \quad \epsilon = \frac{c}{L}, \tag{43}$$

$$\overline{F} = \int_0^1 \left(\frac{\partial \overline{u}_1}{\partial Z}(X,0) - 2N^2 \overline{\omega}(X,0)\right) \mathrm{d}X = \frac{\epsilon}{g_0(\nu + \nu_\gamma)} F. \tag{44}$$

The normalized friction coefficient $\overline{c}_f$ is determined by

$$\overline{c}_f = \frac{\overline{F}}{\overline{W}} = \frac{1}{\epsilon} c_f. \tag{45}$$

The relative viscosity $\overline{\nu}_b$ is defined by

$$\overline{\nu}_b = \frac{\nu_b}{\nu}. \tag{46}$$

From Formula (16), the relation between α and $\overline{\nu}_b$ is

$$\overline{\nu}_b = \frac{1 - \alpha N^2}{1 - N^2}. \tag{47}$$

First, we compute the velocity field $\overline{u}_1$ is given by Eq. 58. We consider its value at the lower boundary $Z = 0$ and we compare it with the value $\overline{s}_1 = 1$ which is the velocity of the wall. Obviously, the slippage effect tends to zero as the parameter δ tends to zero, as shown in Figs. 2–5 for any value $\overline{\nu}_b$. For small values of $\overline{\nu}_b$, there is a retardation effect for all points in the contact so that the effective velocity of the fluid near $Z = 0$ is smaller than the velocity of the wall, namely 1. For increasing values of $\overline{\nu}_b$, the retardation effect is limited to the entrance of the device while the velocity of the fluid near the exit becomes greater than that of the wall. Then, for $\overline{\nu}_b$ greater than the one, the retardation effect disappears. This phenomenon has some direct consequences for the load and the friction coefficient.

In Figs. 6 and 7, we aim to compare the load $\overline{W}$ and friction coefficient $\overline{c}_f$ of the present study with values noted:

- $\overline{W}_2, \overline{c}_{2f}$, obtained by Bessonov [34] making $\delta = 0$.
- $\overline{W}_1, \overline{c}_{1f}$, obtained by classical micropolar analysis with zero value for the microrotation along the solid surface (so making $\delta = 0$ and $\overline{\nu}_b = \frac{1}{1-N^2}$).
- $\overline{W}_0, \overline{c}_{0f}$, related to classical newtonian flow ($\delta = 0, \overline{\nu}_b = 1, N = 0$).

In Fig. 6 we give the normalized load obtained for these various models. As the Newtonian and classical micropolar models do not rely on the parameters δ and $\overline{\nu}_b$, the resulting loads are constant.

As a consequence of the evolution of the slippage effects described previously, the computed load of the slider is lower than that of the Newtonian case for most of the values of the two boundary-condition parameters δ and

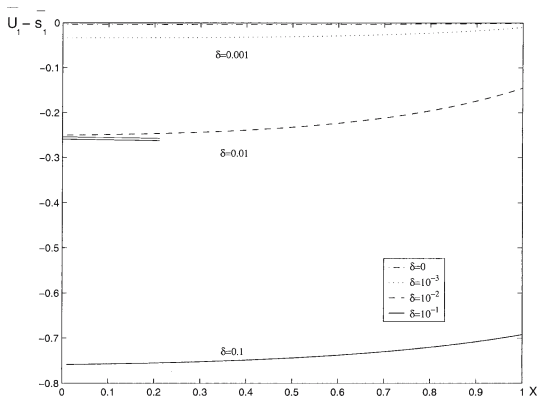

Fig. 2 Slippage value against rescaled variable X for different values of δ, $N = 0.3$ and $R_M = 0.01$ $\overline{\nu}_b = 0.6$

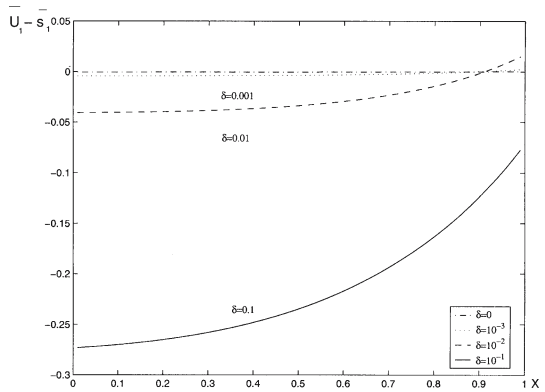

Fig. 3 Slippage value against rescaled variable X for different values of δ, $N = 0.3$ and $R_M = 0.01$ $\overline{\nu}_b = 0.95$

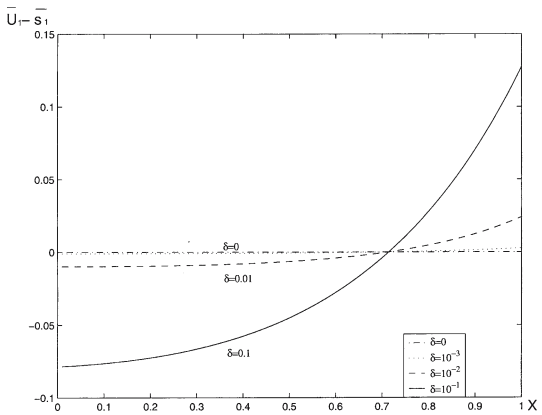

Fig. 4 Slippage value against resaceld variable X for different values of δ, $N = 0.3$ and $R_M = 0.01$ $\overline{\nu}_b = 1$

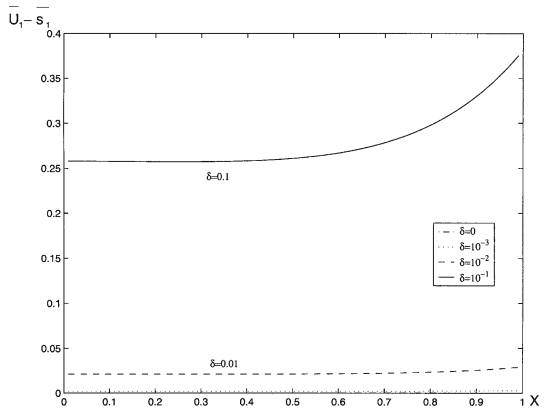

Fig. 5 Slippage value against resaceld variable X for different values of δ, $N = 0.3$ and $R_M = 0.01$ $\overline{\nu}_b = 1.05$

$\overline{\nu}_b$. However, there is a range of values of these parameters for which the load increases, roughly speaking for $\overline{\nu}_b$ between 1 and $1/(1 - N^2)$ and δ smaller than 10^{-2}.

As far as the friction coefficient is concerned, the same difference of behaviour is exhibited (see Fig. 7). The friction coefficient is greater than the Newtonian one with the exception of two parameters ranges: one near $\overline{\nu}_b = 0$, for which the load tends to zero and the other near $\overline{\nu}_b = 1$. For the values δ already mentioned, these lead to an improvement of the load. Figure 8 summarizes these results, making clear the ability to improve both the friction coefficient and load by varying only the boundary conditions of the fluid–surface interface. As a difference with the preceding figures, the micropolar parameter $N = 0.1$ is chosen instead of $N = 0.3$ to show the existence of such a phenomenon, even for a moderate value of N.

3.2 The journal bearing

In this case, the fluid is contained between two cylinders in the domain defined in polar coordinates by

$$H(\theta) = c(1 + \zeta \cos\theta), \quad c > 0,\ 0 < \zeta < 1, 0 \leq \theta < 2\pi, \tag{48}$$

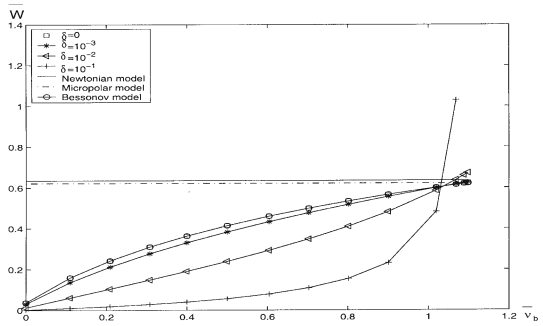

Fig. 6 Normalized load against $\overline{v}_b$ for different values of the slippage parameters δ, for $N = 0.3$ and $R_M = 0.01$

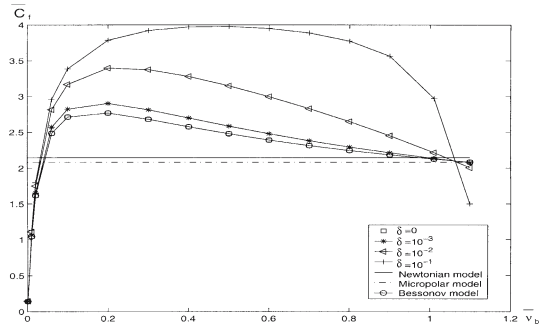

Fig. 7 Normalized friction coefficient against $\overline{v}_b$ for different values of the parameters δ, for $N = 0.3$ and $R_M = 0.01$

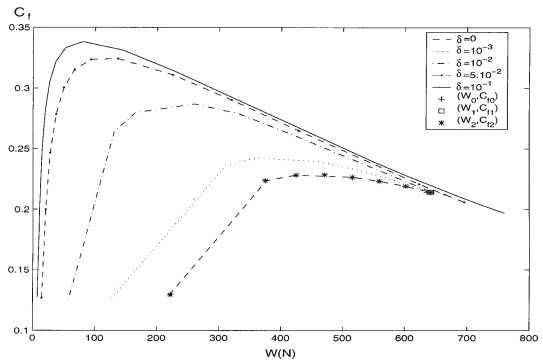

Fig. 8 Real friction coefficients against real loads for different values of δ, for $N = 0.1$ and $R_M = 0.01$ (slider bearing)

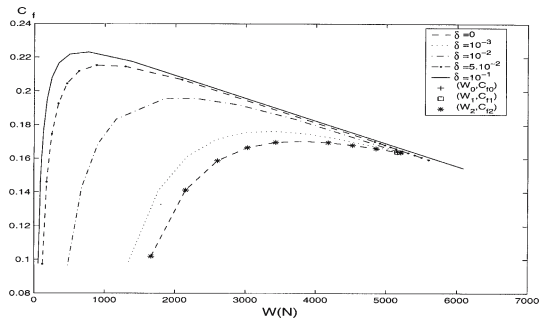

Fig. 9 Real friction coefficients against real loads for different values of δ, $N = 0.1$ and $R_M = 0.01$, $\zeta = 0.5$, $\epsilon = 0.1$, $g_0 = 1\,\text{m/s}$, and $\nu = 10\,\text{kg/m}$ (journal bearing)

where ζ is the eccentricity. Let us also note that, due to the convergent–divergent phase, the solution to the Reynolds equation is negative in the divergent part of the film thickness (cavitation phenomenon) [37]. Various models can be used to take such a phenomenon into account. To compare with [16], We will use the half Sommerfeld boundary-condition model in which the pressure is assumed to be zero for $\theta \geq \pi$. For the computation of W and F we take only the positive part of the pressure.

Due to the circular shape, the load is now given by

$$W = \sqrt{W_n^2 + W_m^2}, \tag{49}$$

where

$$W_n = \int_0^{2\pi} p \cos\theta \,\mathrm{d}\theta \quad \text{and} \quad W_m = \int_0^{2\pi} p \sin\theta \,\mathrm{d}\theta \tag{50}$$

By introducing $X = L\theta$, and $0 < z < H(\theta)$, we may define the friction force by

$$F = L \int_0^{2\pi} \left((\nu + \nu_\gamma) \frac{\partial u_1}{\partial z}(L\theta, 0) - 2\nu_\gamma \omega(L\theta, 0) \right) \mathrm{d}\theta. \tag{51}$$

As with the slider bearing, we aim to compare the results (loads and friction coefficients) obtained by our model with those of [16] (namely W_1, c_{1f}) and [34] (namely W_2, c_{2f}). Although the geometry of the slider and journal bearings are different and in spite of the occurrence of the cavitation phenomenon, numerical results are very similar in both cases. The preceding comments are still valid, as they appear in Fig. 9 where the real load and real friction-coefficient curves are drawn.

4 Conclusions

Whereas the classical no-slip boundary conditions for the velocity are well accepted for usual lubricated devices,this is not the case as the gap between the moving surfaces decreases to molecular dimensions. Various explanations have been proposed to explain the discrepancies between theoretical and experimental results. Some of them address the influence of micro-geometry, while some others point to the interaction between fluid and solid molecules. It has been shown that introducing a new boundary condition at the fluid–solid interface, associated with the existence of a local boundary viscosity, can lead to a mathematical well-posed Stokes problem. However, it has been proved that it is impossible to simultaneously retain a no-slip condition for the velocity on the same interface. A mathematical choice of velocity condition compatible with this new boundary condition has been obtained by using a variational formulation for the Stokes-related problem. This condition allows a slippage in the tangential direction and retains a non-penetration condition in the normal direction. This slippage is proportional to the microrotation field and not to the shear stress as usual. As a direct consequence of the introduction of this no-slip phenomenon, a decrease of the performance of the lubricated devices must be expected. Numerical computations for the two devices show this decrease with the exception of a specific range of the boundary parameters for which both load and friction are improved.

Using the present study as a starting point, various improvements can be proposed. The first one is the generalization of the asymptotic study which leads to the Reynolds equation to a truly nonlinear Navier–Stokes system (and not only Stokes system). In the same way, introducing a time-dependent geometry could be useful to model squeeze experiments in which the upper surface of the device moves downwards. Another possible way is linked to the numerical observation of local improvements of performances for specific values of the parameters. How can this be explained? Can the geometry of the lubricated device be optimized in such a way that this range of parameters be enlarged? Finally, the problem of introducing micro-roughness might be considered for a very small gap, as it is difficult to maintain the assumption of a very smooth function h. Whereas the homogenization multiscale analysis is well established in the lubrication field to get an averaged equation from the classical Reynolds equation when the geometry of the gap performs small periodic oscillations, this is not the case for micro-polar flows. This approach could be very interesting, as it combines both aspects that seem to explain what happens at the interface between fluid and solid, namely micro-roughness and chemical effects.

Appendix 1: Computation of the coefficients of the Reynolds equation ($a \neq 1$)

In this Appendix we describe how to obtain the coefficient of the Reynolds equation (30) from the system (19–29) when the coefficient α differs from 1.

We note that $(\overline{u}_1, \overline{\omega}_2)$ and $(\overline{u}_2, -\overline{\omega}_1)$ satisfy the same equations and boundary conditions by writing $\overline{s}_2$ and Y instead of $\overline{s}_1$ and X. So we describe only the computation of $(\overline{u}_1, \overline{\omega}_2)$. We solve Eqs. 19, 22, (resp. (26), (27)) using the boundary conditions (25), (28) and (29). First, we integrate Eq. 19 with respect to Z to obtain

$$\frac{\partial \overline{u}_1}{\partial Z} = \frac{\partial \overline{p}}{\partial X} Z + 2N^2 \overline{w}_2 + C(X, Y), \tag{52}$$

where C is an unknown function. Putting (52) into (22), we obtain a second-order differential equation

$$\frac{\partial^2 \overline{\omega}_2}{\partial Z^2} - \frac{4N^2}{R_M}(1 - N^2)\overline{\omega}_2 = -\frac{2N^2}{R_M}\frac{\partial \overline{p}}{\partial X} Z - \frac{2N^2}{R_M} C(X, Y), \tag{53}$$

The solution is

$$\overline{\omega}_2 = A(X, Y)\cosh(kZ) + B(X, Y)\sinh(kZ) + \frac{Z}{2(1 - N^2)}\frac{\partial \overline{p}}{\partial X} + \frac{C(X, Y)}{2(1 - N^2)}, \tag{54}$$

where $k = 2N\sqrt{\frac{1-N^2}{R_M}}$ and A and B are unknown functions.

Putting this solution into Eq. 52, we can write $\overline{u}_1$ as follows:

$$\overline{u}_1 = \frac{2N^2}{k}(A(X,Y)\sinh(kz) + B(X,Y)\cosh(kZ)) + \frac{Z}{2(1-N^2)}\frac{\partial \overline{p}}{\partial X} + \frac{C(X,Y)}{1-N^2}Z + D(X,Y). \tag{55}$$

We rewrite C, D, as a function of A and B, using the boundary conditions.

First, using (25), we obtain for $\alpha \neq 1$

$$C(X,Y) = \gamma_\alpha(1-N^2)A(X,Y), \tag{56}$$

where $\gamma_\alpha = \frac{2(1-\alpha N^2)}{\alpha - 1}$.

Using (29) in (55), taking into account (56) and introducing the following split due to the linearity of the system of equations

$$A(X,Y) = A_1(X,Y)\frac{\partial \overline{p}}{\partial X} + A_2(X,Y)\overline{s}_2,\ B(X,Y) = B_1(X,Y)\frac{\partial \overline{p}}{\partial X} + B_2(X,Y)\overline{s}_2. \tag{57}$$

So $\overline{u}_1$ and $\overline{\omega}_2$ are

$$\begin{aligned}\overline{u}_1(X,Y,Z) = &\left[\left(\frac{2N^2}{k}(\sinh(kZ) - \sinh(kH)) + \gamma_\alpha(Z-H)\right)A_1 + \frac{2N^2}{k}(\cosh(kH) - \cosh(kH))B_1\right.\\ &\left. + \frac{Z^2 - H^2}{2(1-N^2)}\right]\cdot\frac{\partial \overline{p}}{\partial X} + \left[\left(\frac{2N^2}{k}(\sinh(kZ) - \sinh(kH)) + \gamma_\alpha(Z-H)\right)A_2\right.\\ &\left. + \frac{2N^2}{k}(\cosh(kZ) - \cosh(kH))B_2\right]\overline{s}_1,\end{aligned} \tag{58}$$

and

$$\begin{aligned}\overline{\omega}_2(X,Y,Z) = &\left[\left(\cosh(kZ) + \frac{\gamma_\alpha}{2}\right)A_1 + \sinh(kZ)B_1 + \frac{Z}{2(1-N^2)}\right]\frac{\partial \overline{p}}{\partial X}\\ &+ \left[\left(\cosh(kZ) + \frac{\gamma_\alpha}{2}\right)A_2 + \sinh(kZ)B_2\right]\overline{s}_1,\end{aligned} \tag{59}$$

where A_i, $B_i\,(i = 1, 2)$ are identified, using boundary conditions (28), and $\overline{\omega}_2(X,Y,H) = 0$

$$A_1(X,Y) = \frac{L(X,Y)}{2(1-N^2)}(H[2N^2(1-\cosh(kH)) + \delta k^2] - k\sinh(kH)[\delta - H^2]), \tag{60}$$

$$A_2(X,Y) = -kL(X,Y)\sinh(kH) \tag{61}$$

$$B_1(X,Y) = \frac{L(X,Y)}{2(1-N^2)}\left(H[2N^2\sinh(kH) + \gamma_\alpha kH] + k[\delta - H^2]\left[\cos(kH) + \frac{\gamma_\alpha}{2}\right]\right), \tag{62}$$

$$B_2(X,Y) = kL(X,Y)\left(\frac{\gamma_\alpha}{2} + \cosh(kH)\right), \tag{63}$$

and

$$L(X,Y) = -\left(\left[\frac{\gamma_\alpha}{2}\cosh(kH)\right][2N^2(1-\cosh(kH)) + \delta k^2] + \sinh(kH)[\gamma_\alpha kH + 2N^2\sinh(kH)]\right)^{-1}. \tag{64}$$

Similarly, we obtain, using (26), (27) and (29),

$$\begin{aligned}\overline{u}_2(X,Y,Z) = &\left[\left(\frac{2N^2}{k}(\sinh(kZ) - \sinh(kH)) + \gamma_\alpha(Z-H)\right)A_1 + \frac{2N^2}{k}(\cosh(kZ) - \cosh(kH))B_1\right.\\ &\left. + \frac{Z^2 - H^2}{2(1-N^2)}\right]\cdot\frac{\partial \overline{p}}{\partial Y} + \left[\left(\frac{2N^2}{k}(\sinh(kZ) - \sinh(kH)) + \gamma_\alpha(Z-H)\right)A_2\right.\\ &\left. + \frac{2N^2}{k}(\cosh(kZ) - \cosh(kH))B_2\right]\overline{s}_2,\end{aligned} \tag{65}$$

$$\begin{aligned}\overline{\omega}_1(X,Y,Z) = &-\left[\left(\cosh(kZ) + \frac{\gamma_\alpha}{2}\right)A_1 + \sinh(kZ)B_1 + \frac{Z}{2(1-N^2)}\right]\frac{\partial \overline{p}}{\partial Y} - \left[\left(\cosh(kZ) - \frac{\gamma_\alpha}{2}\right)A_2\right.\\ &\left. + \sinh(kZ)B_2\right]\overline{s}_2.\end{aligned} \tag{66}$$

Appendix 2: Computations of the coefficients of the Reynolds equation ($a = 1$)

In this Appendix we describe how to obtain the coefficient of the Reynolds equation (30) from the system (19–29) as the coefficient $\alpha = 1$.

$$\overline{u}_1(X,Y,Z) = \left[\frac{A_1'}{1-N^2}(Z-H) + \frac{2N^2}{k}(\cosh(kZ)-\cosh(kH))B_1' + \frac{Z^2-H^2}{2(1-N^2)}\right]\frac{\partial \overline{p}}{\partial X} \tag{67}$$

$$+\left[\frac{A_1'}{1-N^2}(Z-H) + \frac{2N^2}{k}(\cosh(kZ)-\cosh(kH))B_2'\right]\overline{s}_1, \tag{68}$$

$$\overline{\omega}_2(X,Y,Z) = \left[\frac{A_1'}{1-N^2} + \sinh(kZ)B_1' + \frac{Z}{2(1-N^2)}\right]\frac{\partial \overline{p}}{\partial X} + \left[\frac{A_2'}{2(1-N^2)} + \sinh(kZ)B_2' + \right]\overline{s}_2, \tag{69}$$

$$\overline{u}_2(X,Y,Z) = \left[\frac{A_1'}{1-N^2}(Z-H) + \frac{2N^2}{k}(\cosh(kZ)-\cosh(kH))B_1' + \frac{Z^2-H^2}{2(1-N^2)}\right]\frac{\partial \overline{p}}{\partial Y} \tag{70}$$

$$+\left[\frac{A_2'}{1-N^2}(Z-H) + \frac{2N^2}{k}(\cosh(kZ)-\cosh(kH))B_2'\right]\overline{s}_2, \tag{71}$$

$$\overline{\omega}_1(X,Y,Z) = -\left[\frac{A_1'}{2(1-N^2)} + \sinh(kZ)B_1' + \frac{Z}{2(1-N^2)}\right]\frac{\partial \overline{p}}{\partial Y} - \left[\sinh(kZ)B_2' + \frac{A_2'}{2(1-N^2)}\right]\overline{s_2}, \tag{72}$$

where

$$A_1'(X,Y) = L'(X,Y)(H[2N^2(1-\cosh(kH)) + \delta k^2] - k\sinh(kH)[\delta - H^2]), \tag{73}$$

$$A_2'(X,Y) = -2(1-N^2)kL'(X,Y)\sinh(kH), \tag{74}$$

$$B_1'(X,Y) = \frac{L'(X,Y)}{2(1-N^2)} + (\delta + H^2)k, \tag{75}$$

$$B_2'(X,Y) = kL'(X,Y) \tag{76}$$

with

$$L'(X,Y) = -(2N^2(1-\cosh(kH)) + \delta k^2 + 2Hk\sinh(kH))^{-1}. \tag{77}$$

we note that, as α tends to unity, L tends to zero, while $\frac{\gamma_\alpha}{2}L$ tends to L'. Hence it is easily verified that

$$A_1, A_2 \longrightarrow 0, B_1 \longrightarrow B_1' \quad \text{and} \quad B_2 \longrightarrow B_2', \tag{78}$$

while

$$\gamma_\alpha A_1 \longrightarrow \frac{A_1'}{1-N^2}, \quad \gamma_\alpha A_2 \longrightarrow \frac{A_2'}{1-N^2}. \tag{79}$$

References

1. Hartl M, Krupka I, Liska M (1999) An automatic system for real-time evaluation of EHD film thickness and shape based on the colorimetric interferometry. Tribol Trans 42(2):303–309
2. Hartl M, Krupka I, Poliscuk R, Liska M, Molimard J, Querry M, Vergne P (2001) Thin film colorimetric interferometry. Tribol Trans 44(2):270–276
3. Johnston GJ, Wayte R, Spikes HA (1991) The measurement and study of very thin lubricant films in concentrated contacts. Tribol Trans 34(2):187–194
4. Luo JB, Wen SZ (1996) Mechanism and characteristics of thin film lubrication at nanometer scale. Science China (A) 39(12):1312–1322

5. Luo JB, Huang P, Wen SZ (1996) Thin film lubrication part I: study on the transistion between EHL and thin film lubrication using relative optical interference intensity technique. Wear 194:107–115
6. Luo JB, Huang P, Wen SZ, Lawrence L (1999) Characteristics of fluid lubricant films at the nano-scale. ASME Trans 2121(4):872–878
7. Shen MW, Luo JB, Wen SZ (2001) The tribological properties of oils added with diamond nano-particles. Tribol Trans 44(3):494–498
8. Aero EL, Bessonov NM (1989) Micromechanics of structural liquid layers between solids in contact. Advances in Science and Technology of VINITI (Itogi Nauki i Tekniki VINITI (USSR)) Serie Mechanics of fluids and Gases 1989, 23, pp 237–315
9. Derjaguin BV, Karasev VV, Lavigin IA, Shorochodov I, Chromova EN (1972) Research of boundary viscosity of the dimethylsiloxane oligomers. Surface forces in thin films and dispersion system. Nauka M, USSR pp 209–214
10. Eringen AC (1964) Simple micro fluid. Int J Engng Sci 2:205–217
11. Eringen AC (1966) Theory for micropolar fluid. J Math Mech 16(1):1–16
12. Aero EL, Bulygin AN, Kuvshinskii EV (1965) A Symmetric hydromechanics. J Appl Math Mech 29(2):297–308 (Russian)
13. Łukaszewicz G (1999) Micropolar fluids, theory and applications. Modelling and simulation in science, engineering and technology, Birkhäuser, Boston
14. Allen SJ, Kline KA (1972) Lubrication theory for micropolar fluids. J Appl Mech 38:834
15. Agrawal VK, Ganju KL, Jethi SC (1972) Squeeze film and externally pressurized bearing micropolar fluid. Wear 19:217
16. Prakash J, Sinha P (1975) Lubrication theory of micropolar fluids and its application to a journal bearing. Int J Engng Sci 13: 217–232
17. Shukla JB, Isa M (1975) Generalized Reynolds equation for micropolar lubricants and its application to optimum one-dimensional slider bearings: effects of solid particle additives in solution. J Mech Engng Sci 17(5):280–284
18. Tipei N (1979) Lubrication with micropolar liquids and its application to short bearings. J Lubr Technol 101:356–363
19. Bessonov NM (1993) Boundary viscosity conception in hydrodynamical theorey of lubrication. Preprint 81, Russian Academy of Sciences, Institute of the problems of Mechanical Engineering, St-Petersbourg
20. Lauga L, Brenner MP, Stone HA. Microfluidics: the no-slip boundary condition. In: Foss I, Tropea C, Yarin A (eds) Handbook of experimental fluid dynamic. Springer, New-York
21. Migun NP (1984) On hydrodynamic boundary conditions for microstructural fluids. Rheologica Acts 23(6):575–581
22. Prokhorenko PP, Migun NP, Grebenshchicov SV (1987) Experimental studies of polar indicator liquids used in capillary penetrant testing. Int J Engng Sci 25(5):482–489
23. Benhaboucha N (2003) Quelques problèmes mathématiques relatifs à la modélisation des conditions aux limites fluide–solide pour des écoulements de faible épaisseur. Thèse 145, Université lyon1, France
24. Bair S, Winer WO (1979) Shear strength measurements of lubricants at high pressure. ASME, Ser F, J Lubr Technol 101(3):251–257
25. Hatzikiriakos SG, Delay JM (1991) Wall slip of molten high density polyethylene I – sliding plate rheometer studies. J Rheol 35:497–523
26. Jacobson BO, Hamrock BJ (1984) Non-Newtonian fluid model incorporated into elastohydrodynamic lubrication of rectangular contacts. ASME J Lubr Technol 106:275–282
27. Meng YG, Zheng J (1999) A rheological model for lithium lubricating grease. Trobol Int 31:619–682
28. Spikes HA (2003) The half-wetted bearing. Part 1: extended Reynolds equation. J Engng Tribol 217:1–14
29. Wilson WD, Huang XB (1989) Viscoplastic behavior of silicone oil in a metalforming inlet zone. ASME. J Tribol 111:585–590
30. Bonaccurso E, Butt HJ, Craig VS (2003) Surface roughness and hydrodynamic boundary slip of a Newtonian fluid in a completely wetting system. Phys Rev Lett 90:144501
31. Craig VSJ, Neto C, Williams DRM (2001) Shear-dependent boundary slip in a aqueous Newtonian liquid. Phys Rev Lett 8705:art. (054504)
32. Kaneta N (1990) Observation of wall slip in elastohydrodynamic lubrication. ASME J Tribol 106:275–282
33. Hervet H, Pit R, Leger L (1999) Friction and slip of a simple liquid at a solid surface. Tribol Lett 7:147–152
34. Bessonov NM (1994) A new generalization of the Reynolds equation for a micropolar fluid and its application to bearing theory. Tribol Int 27(2):105–108
35. Jacobson BO (1997) At the boundary between lubrication and wear. In: Hutchings IM (ed) First world tribology conference. Mech Eng Pub, London pp 291–298
36. Léger L, Hervet H, Pit R (2001) Friction and flow with slip at fluid–solid interfaces, in interfacial properties on the submicron scal. ACS symposium series 781, ACS, Washington DC, Chap. 10, pp 154–167
37. Bayada G, Chambat M (1986) Some modelling of the cavitation regon in hydrodynamic lubrication. J Theor Appl Mech 5(5): 703–729